

# Structure function results from H1

ZHIQING ZHANG<sup>a</sup>

On behalf of the H1 Collaboration

*Laboratoire de l'Accélérateur Linéaire, IN2P3-CNRS et  
Université de Paris-Sud, BP 34, 91898 Orsay Cedex*

## Abstract

New structure function results from H1 are presented. The measurements cover a huge kinematical range for  $Q^2$ , the four momentum transfer squared, from  $0.35 \text{ GeV}^2$  to  $30\,000 \text{ GeV}^2$ , and for Bjorken  $x$  between  $\sim 5 \cdot 10^{-6}$  and  $0.65$ . At  $Q^2 > 100 \text{ GeV}^2$ , full HERA I data have been analyzed. The data are compared with a new QCD analysis. The impact of the HERA I data on the parton density functions is discussed.

---

<sup>a</sup>zhangzq@lal.in2p3.fr

# 1 Introduction

Deep inelastic scattering (DIS) experiments have played an important role in the understanding of the partonic structure of matter and in establishing the strong interaction sector of the Standard Model (SM): QCD.

In the past decade, the HERA experiments H1 and ZEUS have been providing more and more precise data for modern global fits allowing parton density functions (PDFs) be determined with steadily increasing precision. The precision of the PDFs is of importance as it is needed to have reliable predictions for precision measurements and for new physics searches at future hadron colliders such as LHC.

In this talk, I shall first present the latest new structure function measurements from H1, then try to answer two following questions: i) Can HERA I cross section or structure function (SF) data measured so far be described by QCD? and ii) What is the impact of the HERA I data?

## 2 New Measurements and Impact of HERA I Data

Four new preliminary measurements [1] from H1 have been submitted to this conference. Thanks to the increased proton beam energy from 820 GeV to 920 GeV since 1998 (the center-of-mass energy  $\sqrt{s}$  is accordingly increased from 300 GeV to 320 GeV), the fully installed backward silicon tracker, the new capability of triggering low energy scattered electrons<sup>1</sup> down to 3 GeV, and the special runs where data were taken by shifting the nominal interaction vertex in the proton beam direction by 70 cm, the kinematical domain has been substantially extended with respect to previous measurements both to lower  $Q^2$  and to smaller  $x$ . On the other extreme at high  $Q^2$  and large  $x$ , the new measurements of both neutral current (NC) and charged current (CC) processes are obtained with improved precision using the highest data sample taken before the HERA machine was upgraded for the second phase.

Part of the new measurements at low  $Q^2$ , the so-called reduced cross sections  $\tilde{\sigma}$  (or  $\sigma_r$ ), are shown in Fig. 1. The reduced cross section for the NC interaction may be expressed in terms of SFs as

$$\tilde{\sigma}_{\text{NC}}(e^\pm p) = F_2 - \frac{y^2}{Y_+} F_L \mp \frac{Y_-}{Y_+} x F_3 \quad (1)$$

where  $Y_\pm = 1 \pm (1 - y)^2$  with  $y = Q^2/(xs)$ ,  $F_2$  is the dominant contribution, the contribution of the longitudinal SF  $F_L$  is suppressed at low  $y$  by  $y^2/Y_+$ , and the SF  $x F_3$ , which arises mainly from the photon- $Z^0$  interference and has been previously determined [5] at  $Q^2 \geq 1500 \text{ GeV}^2$ , becomes non-negligible only at such large  $Q^2$  values. The reduced cross section differs from the experimentally measured double differential cross section  $d^2\sigma/dxdQ^2$  by a kinematical factor of  $2\pi\alpha^2 Y_+/xQ^4$ , where  $\alpha$  is the fine structure constant.

From Fig. 1, one observes that the new measurements extend now down to  $x \sim 5 \cdot 10^{-6}$  at  $Q^2 = 0.35 \text{ GeV}^2$ . The rise of  $F_2$  as  $x$  decreases, the first important observation at HERA and being related to increasing gluon density  $xg$  at small  $x$ , persists even at  $Q^2 < 1 \text{ GeV}^2$

---

<sup>1</sup>It refers generically to both electrons and positrons unless stated otherwise.

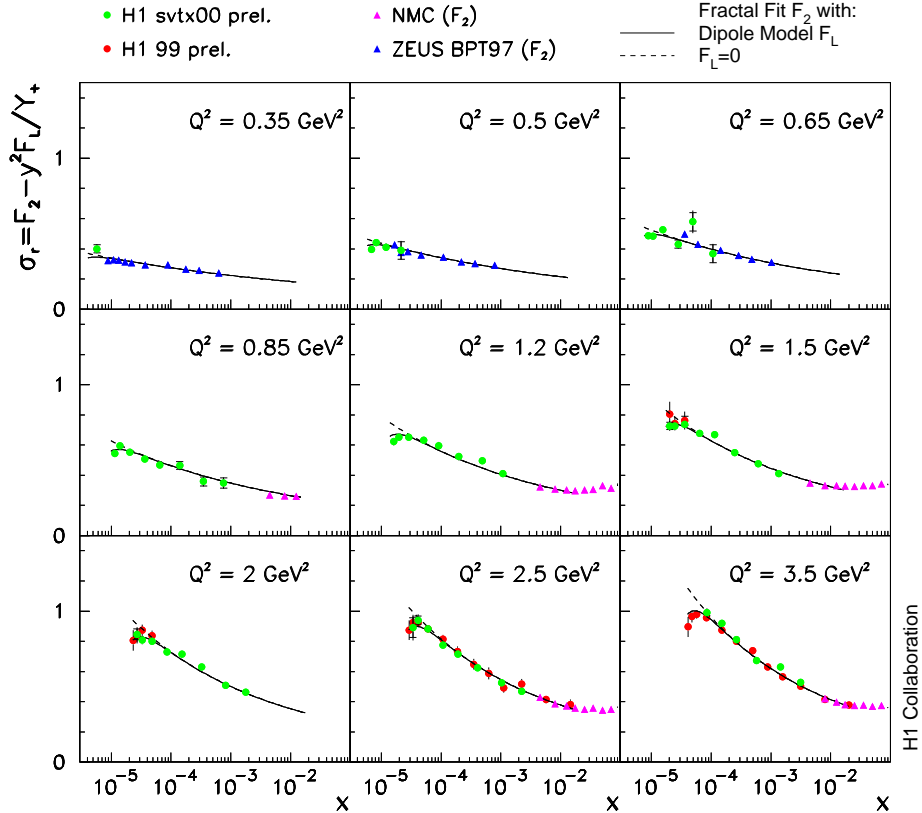


Figure 1: Preliminary reduced cross section (see text) measurements from H1 shown as a function of  $x$  for  $Q^2 \leq 3.5 \text{ GeV}^2$ . Also shown are measurements from NMC [2] and ZEUS [3] and expectations based on a phenomenological model [4].

although with a reduced magnitude. The same observation is also obtained from the measurement of  $d \ln F_2 / d \ln x$  (not shown here).

As  $Q^2$  increases, the measured  $\sigma_r$  is observed to deviate from the dashed curves at high  $y$  in which the  $F_L$  is set to zero, but agree with the full curves where a non-zero  $F_L$  according to a dipole model is included. Such a sensitivity to  $F_L$  has been exploited by H1 to determine experimentally  $F_L$ , which is shown in Fig. 2. The new determination (shown in triangle) thus extends the previous determination [6] to smaller  $x$  and higher  $Q^2$ . It should be pointed out that such a determination, though not a direct measurement which needs different beam energies, does provide a non-trivial consistency test as the determination gives a direct measure of  $xg$  while the expectation from a QCD fit was based on an indirect  $xg$  derived from the scaling violation of the  $F_2$ .

Moving to even higher  $Q^2$  (100–30 000  $\text{GeV}^2$ ) region, new preliminary cross section measurements based on the  $e^+p$  1999–2000 at  $\sqrt{s} = 320 \text{ GeV}$  [1] are combined with those measured with the  $e^+p$  1994–1997 at 320  $\text{GeV}$  [8] taking into account a small correction due to the increased  $\sqrt{s}$ . The combined cross sections in  $e^+p$  scattering can be compared with those in  $e^-p$  scattering [5]. In Fig. 3, the single differential NC and CC cross sections from H1 [1, 5] and ZEUS [10, 5] are shown and compared with the SM expectation from a global QCD fit (CTEQ5 [9]). While the NC  $e^+p$  and  $e^-p$  cross sections are indistinguishable

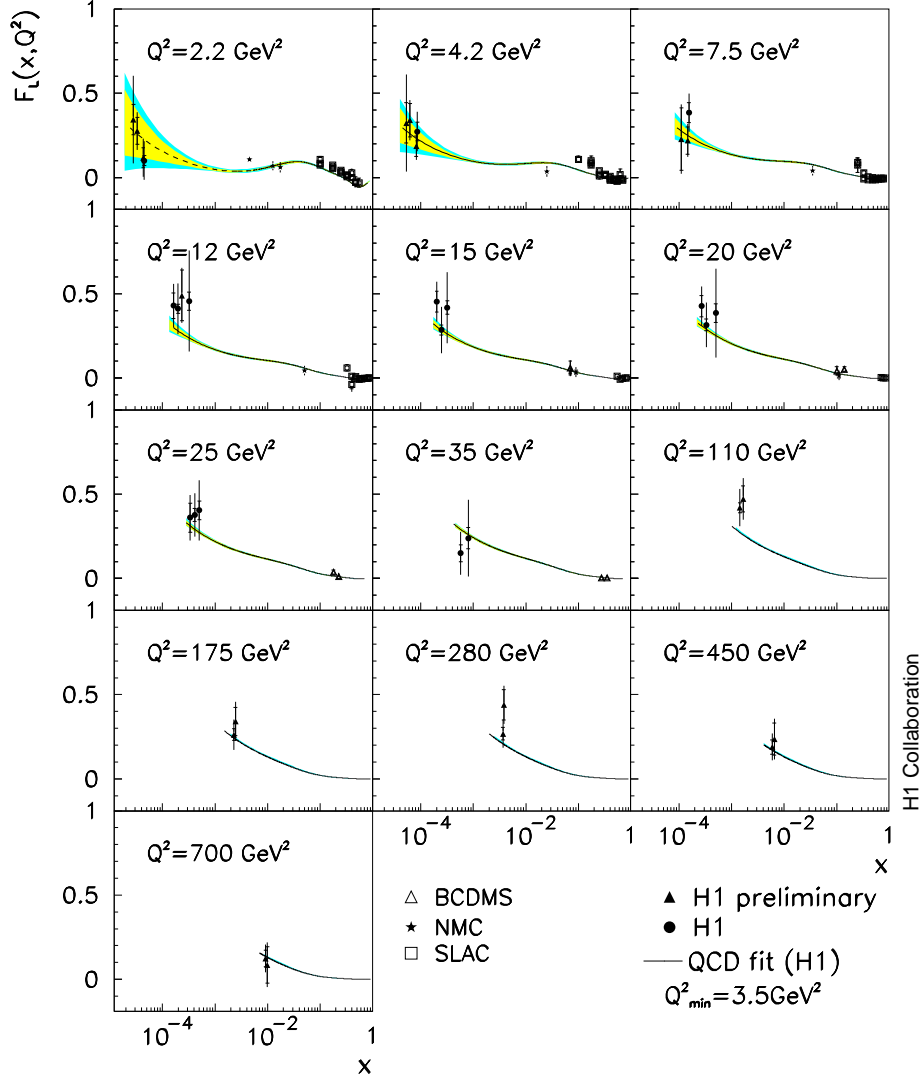


Figure 2: Preliminary determination of  $F_L$  shown together with those by H1 [6] and BCDMS, NMC, and SLAC [7]. Also shown is the SM expectation - QCD fit (H1) [6].

at low  $Q^2$  as expected from the photon ( $\gamma$ ) exchange, they are different at high  $Q^2$  due to the positive (negative)  $\gamma Z^0$  exchange in  $e^-p(e^+p)$  interactions. The CC  $e^+p$  and  $e^-p$  cross sections are different over the entire  $Q^2$  region measured originating from different quarks probed by negatively and positively charged W bosons exchanged in the interactions and from different helicity structures involved. At  $Q^2 \sim M_{Z,W}^2$ , all four cross sections (NC, CC and  $e^+p$ ,  $e^-p$ ) are comparable demonstrating the universal coupling strength of electroweak interactions. It is also remarkable that the cross sections which vary over many orders of magnitude are described by the global fit which to some extent is independent of the data.

HERA data have been important for constraining the gluon density  $xg$  at small  $x$ . Indeed, in an earlier QCD analysis performed by H1 using the H1 low  $Q^2$  precision data and part of the H1 high  $Q^2$   $e^+p$  data available then, the gluon density  $xg$  was determined with an experimental precision of about 3% [6]. In addition, the strong coupling constant

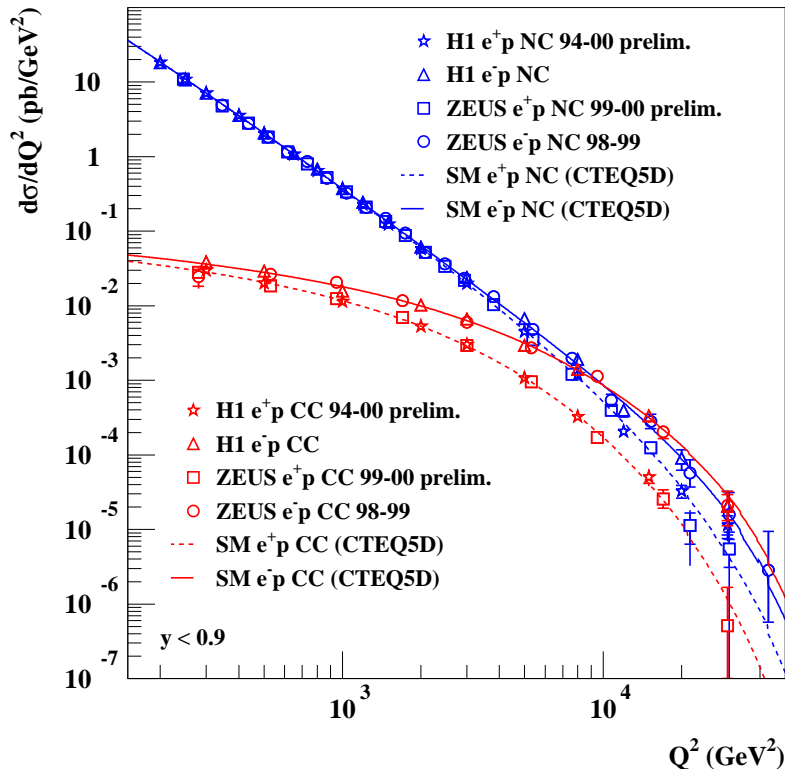


Figure 3: NC and CC cross sections  $d\sigma/dQ^2$  measured with  $e^+p$  and  $e^-p$  data by H1 [1, 5] and ZEUS [10, 5] in comparison with the SM expectations from CTEQ5 [9].

$\alpha_s$  was determined with an experimental uncertainty of 1.5% [6] using the same data together with the proton data from BCDMS [11] for constraining  $xg$  at large  $x$ . This determination at next-to-leading order (NLO) is unfortunately limited theoretically by the large scale uncertainty showing the necessity of having next-to-NLO calculations for improvements.

Presented at this conference is a further NLO QCD analysis performed by H1 using the low  $Q^2$  precision data and all high  $Q^2$  cross section data. The analysis aims at a determination of the quark momentum distributions, besides  $xg$ . A novel feature of the analysis is the way in which the various structure functions are decomposed in terms of different parton densities. The quark densities used by H1, the upper and down types of quarks ( $xU$ ,  $xD$ ) and their anti-quarks ( $x\bar{U}$ ,  $x\bar{D}$ ), directly enter the NC and CC cross sections contrary to an effective sea distribution or valence quark distributions. The latter follow from the differences  $u_v = U - \bar{U}$  and  $d_v = D - \bar{D}$ . The initial distributions are parametrized in an MRST-like functional form for  $Q_0^2$  at  $4\text{ GeV}^2$ . The results of the fit are shown in Fig. 4 as a function of  $x$ . In the fit with the full HERAI data plus the BCDMS proton and deuterium data [11], the experimental uncertainty shown in dark error band reaches a precision of a few percent. Shown in light error band is the model uncertainty, which includes variation of  $Q_0^2$  and other parameters in the fits. The results of the fit using the H1 data only is shown with the solid curves. It is remarkable that the fit using HERA data only is able to give consistent results on the parton density

functions with the combined fit which uses additional data at low  $Q^2$  and large  $x$ .

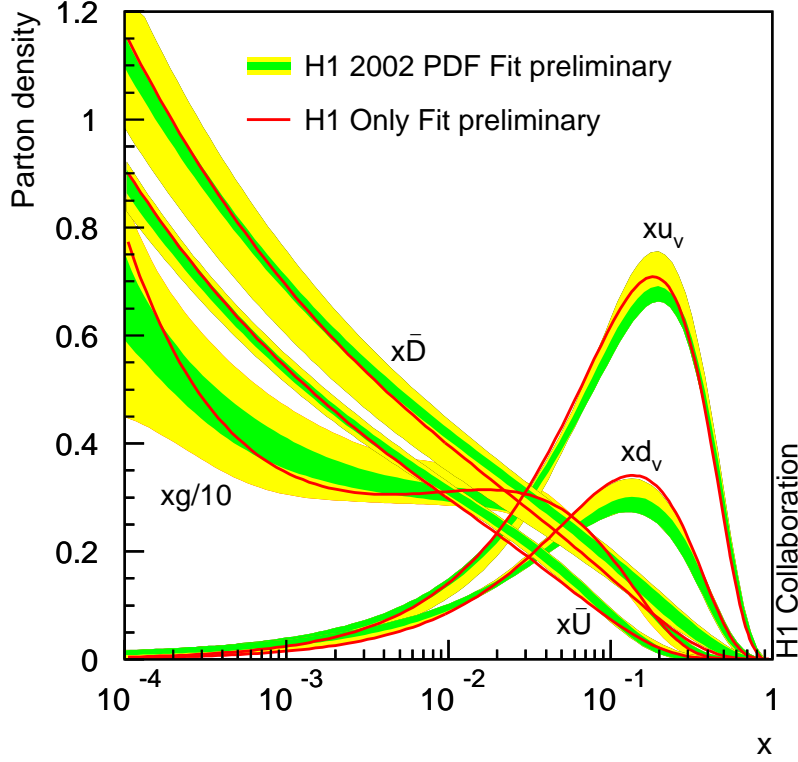


Figure 4: The valence quark densities  $xu_v, xd_v$ , the anti-up and down type densities  $x\bar{U}, x\bar{D}$  and the gluon density  $xg$  (reduced by a factor of 10), from the combined fit (error bands) using the H1 and BCDMS data [11] are compared with those from the fit (solid curves) using the H1 data only.

The impact of the HERA I data at large  $x$  is best seen on the  $u$  and  $d$  quark densities at valence quark region, determined by two complementary methods (Fig. 5). In one method, the densities are determined from the fit, where the precision is optimal, while in the second method, the densities ( $xq_{\text{exp}}$ ) are extracted locally from the measured cross sections  $\tilde{\sigma}_{\text{meas}}(x, Q^2)$ ,  $xq_{\text{exp}} = \tilde{\sigma}_{\text{meas}}[xq/\tilde{\sigma}]_{\text{fit}}$ . The latter method has the advantage that the resulting  $u$  and  $d$  densities do not depend on the  $Q^2$  evolution and are thus free from any nuclear corrections.

### 3 Conclusion

To conclude, the structure function data from almost a decade's operation in HERA phase I have enabled the theory of QCD be tested to a new level of precision in deep inelastic scattering and revealed its impact on the parton densities both for the gluon at small  $x$  and for the  $u$  and  $d$  at large  $x$ . The full HERA I data at large  $x$  and high  $Q^2$  are still statistically limited. New data to be taken during the next years in HERA phase II are therefore important not only to improve the precision of the structure functions but also to fully explore the very high  $Q^2$  region up to the kinematical limit  $s \sim 10^5 \text{ GeV}^2$ .

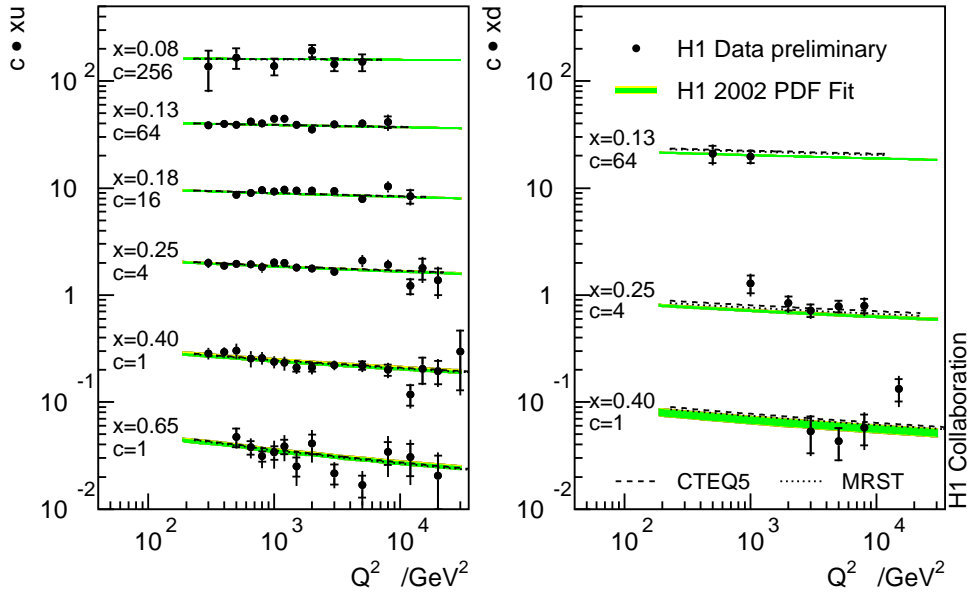


Figure 5: The  $u$  and  $d$  quark densities determined from the local extraction method (full points) and from the fit are compared with those from CTEQ5 [9] and MRST [12]. For displaying purpose, the densities are multiplied by a factor  $c$ .

## References

- [1] H1 Collab., “A new measurement of the DIS cross section and of  $F_L$  at low  $Q^2$  and Bjorken  $x$  at HERA”, contribution paper # 799;  
 “Measurement of the inclusive DIS cross section at  $Q^2 \sim 1 \text{ GeV}^2$  with the H1 experiment”, contribution paper # 975;  
 “Measurement of the proton structure function using radiative events at HERA”, contribution paper # 976;  
 “Measurement of inclusive DIS at high  $Q^2$  and large  $x$ ”, contribution paper # 978.
- [2] NMC Collab., A. Arneodo et al., Phys. Lett. **B364** (1997) 107, Nucl. Phys. **B483** (1997) 3.
- [3] ZEUS Collab., J. Breitweg et al., Phys. Lett. **B487** (2000) 53.
- [4] T. Lastovicka, hep-ph/0203260.
- [5] H1 Collab., C. Adloff et al., Eur. Phys. J. **C19** (2001) 269;  
 ZEUS Collab., DESY-02-113.
- [6] H1 Collab., C. Adloff et al., Eur. Phys. J. **C21** (2001) 33.
- [7] BCDMS Collab., A. C. Benvenuti et al., Phys. Lett. **B223** (1989) 485;  
 NMC Collab., second reference of [2];  
 L. W. Whitlow et al., Phys. Lett. **B250** (1990) 193.
- [8] H1 Collab., C. Adloff et al., Eur. Phys. J. **C13** (2000) 609.

- [9] CTEQ Collab., <http://www.phys.psu.edu/~cteq>.
- [10] ZEUS Collab., J. Breitweg et al., Eur. Phys. J. **C11** (1999) 427, **C12** (2000) 411.
- [11] BCDMS Collab., first reference of [7].
- [12] A. D. Martin et al., Eur. Phys. J. **C4** (1998) 463.